

MULTI CLASSIFICATION OF BRAIN TUMOUR MRI IMAGES USING DEEP CONVOLUTIONAL NEURAL NETWORK

Dr S Sasipriya Ph.D¹ M Benedict Tephila² S Sanjana³ M Indirapriyadharshini⁴

¹Professor, ²Assistant Professor, ^{3,4}PG Student

Department of Electronics and Communication Engineering, Sri Krishna college of Engineering and Technology, Coimbatore

Abstract - Today, cancer poses a serious threat to human life. The phases of a brain tumor are varied. One of the prevalent types of tumors that has a relatively high mortality rate globally is the brain tumor. Early detection and prediction of brain tumors is the strongest defense against them. The nature of the corona virus, in which the majority of viruses overlap with one another, makes it difficult to detect brain tumors in their early stages. Based on how similar they are, photographs are grouped together using a computer process. Wavelet transformation is employed in this case to preprocess photos, along with feature extraction and convolutional neural networks, to determine whether a patient's condition is normal or abnormal at an early stage. Performance is determined by the classifier's correct and wrong classifications.

I. INTRODUCTION

The role of brain tumor alterations in neurological diseases is becoming more well-acknowledged, and these changes may open up interesting new therapeutic possibilities. It is crucial to create new techniques for tracking brain tumors as the disease progresses and as they respond to treatment, but this process is still difficult because we can't easily collect brain tissue. The critical requirement for non-invasive evaluation of brain

tumors is starting to be addressed by new neuroimaging techniques. By enabling the in vivo capture of dynamic Brain Tumor data, hyperpolarized ¹³C MRS/magnetic resonance spectroscopic imaging (MRSI; see glossary) is a new method that offers unmatched insights into the in vivo Brain Tumor condition of the organ of interest. Using thermal ¹³C MRS and ¹H, clinical data on steady state human brain tumors have been gathered. These techniques aren't frequently employed in medical settings, though, and thermal ¹³C MRS in particular needs lengthy scan periods and substrate injections to be effective. Brain tumor imaging has benefited from the novel information provided by hyperpolarized ¹³C MRS.

Hyperpolarization of a chemical increases its magnetic resonance imaging (MRI) detectability by more than 10,000 times because of the enhanced signal-to-noise ratio. Summarizes the common procedures of a preclinical hyperpolarized ¹³C MRS/I investigation. Given that the hyperpolarized state only persists for a brief period in solution (known as the relaxation time, or T1), injection into the target biological system (cells, an animal model, or a person) must be quick (10–15 s in animals) and timed to coincide with data collection. The resonances of the injected substrate and its

subsequent Brain Tumor products can subsequently be observed in ^{13}C MR spectra (slab, 2D or 3D, single time point or dynamic), which are obtained using standard MR apparatus. The resonances of hyperpolarized lactate, hyperpolarized alanine, and, in some cases, hyperpolarized ^{13}C bicarbonate are seen in the living brain after injection of hyperpolarized Brain Tumor, the most widely used probe. These resonances represent enzymatic conversion via lactate dehydrogenase (LDH), alanine aminotransferase (ALT), and Brain Tumor dehydrogenase (PDH), respectively. The creation of numerous additional injectable chemicals will be covered later. The hyperpolarized data can then be used to provide MR spectra that show the area(s) under the curve(s), corresponding Brain Tumor ratios of product: substrate (for example, lactate: Brain Tumor), or kinetic pseudo-rate constants for substrate to product conversion. Preclinical models can be used to validate hyperpolarized ^{13}C Brain Tumor data by comparison to more widely used clinical imaging techniques or through correlation analyses with 'ground truth' *ex vivo* biochemical investigations to determine the method's additional value. Clinically, given the rarity of human brain tissue biopsy samples, hyperpolarized ^{13}C MRS/I can offer access to Brain Tumor information that is otherwise inaccessible. Clinical research are currently being conducted in both cancer and cardiovascular illness, where hyperpolarized ^{13}C MRS/I has predominantly been used in the past. The progression of the disease and the effects of treatment have been documented in brain tumor changes in preclinical models of neurological diseases and Neuro-inflammation. Since hyperpolarized ^{13}C MRS/I has already been applied to the clinic, this novel investigation direction of neurological illnesses may enhance our understanding of *in vivo* brain tumors not only pre-clinically but also in patient populations. In this

study, we explore potential directions for future research as well as a summary of hyperpolarized ^{13}C MRS/I's existing applications in the non-oncological neurological field.

II. RELATED WORK

In order to detect cancerous nodules in CT images, Roozgard et al. presented the kernel RX-algorithm, a nonlinear anomaly detector. The RX-algorithm has been successfully used in military imaging applications where malignant nodule detection is quite similar to anomaly detection. They altered the original RX-algorithm to allow it to be used for CT image anomaly detection. They also transferred the data to a high-dimensional space using the kernel method to produce a kernelized RX-algorithm that performs better than the original RX-algorithm. The kernel RX-algorithm has been applied to annotated public access databases, and preliminary findings show that it may be able to detect cancerous nodules early. The disadvantage is that prior knowledge of the image is required, specifically the maximum threshold distance between clusters or the expected number of clusters, k .

When conducting a thorough analysis of medical data, experienced practitioners can benefit from the usage of computerized systems. The brain CAD system focuses on identifying nodules, which can be either benign or cancerous, as potential anomalies. This article examines the methods used by CAD systems in the biomedical image processing field to identify aberrant cell development in the brains. The most widely used CAD Programmes, such as AutoCad, ProgeCAD, and microstation, are expensive for people to purchase. As an alternative, people can attempt the free open source CAD drafting programmes QCAD ([link leaves site](#)), LibreCAD ([link leaves site](#)), and OpenSCAD ([link leaves site](#)). Operators are required to upgrade their

abilities with each new release of the CAD programme. The incorrect use of blocks and layers makes it difficult for another individual to update and modify the designs.

An active appearance model formulation is used to create intensity models of the nodules. A similarity score between the AAM template and the input image is calculated using template matching. To improve nodule detection, it is necessary to maximize the similarity measure at various image pixels. Rotational variations are not taken into consideration by conventional template matching. As an energy optimization problem, our suggested template matching method computes a transformation that incorporates rotation(s) parameters as well as the AAM weighting factors. Because it can manage the changes in rotation between the template and the input images, the method is adaptable to different scans and different nodule sites. The method can use a variety of similarity metrics. Three similarity metrics from the literature—NCC, ZNCC, and ZSSD—will be used in the experiments to demonstrate the effectiveness of the suggested methodology. A clinical study with known ground truth is used to build ROC curves for different types of nodules, which demonstrate appreciable improvements over classic parametric nodule models and template matching criteria. The stylus must remain in constant touch with the surface, which makes it vulnerable to breakage and smudges.

In the early stages of brain cancer, there are frequently no symptoms or warning signals. When evaluating a cough or chest pain, chest x-rays or Computed Tomography (CT) scans are frequently the first to raise a suspicion. A number of studies have been conducted with the goal of developing Computer Aided Diagnosis (CAD) systems that improve the early detection of brain cancer nodules. Using a template matching algorithm combined with

a multi-resolution feature analysis technique, a CAD system is being created to more accurately identify pulmonary brain nodules from Low Dose CT (LDCT) scan pictures. 165 nodules out of 134 were accurately identified. The detection rate as a result is 81.212%. Depending on the system employed, the number of detectors purchased, etc., the initial cost may be substantial. Depending on the team members' degree of computer literacy, mastering the software can take some time. Both the detectors and the phosphor plates cannot be sterilized or autoclaved, and because of their size and rigidity, CCD/CMOS detectors can have positioning issues.

III. PROPOSED SYSTEM

Employing mathematical morphological techniques to create MRI images of the brain, The patient's chance of survival can be significantly increased by early detection and treatment of brain tumors. One of the crucial steps in analyzing medical images is segmentation; in the proposed work, ASM segmentation is used. With the aid of the median filter, pre-processing is done to get rid of the speckle noise, and the mean filter boosts the contrast of the image. Chanvase active contour processing is used for tumor localization. It uses a CNN-based classification algorithm and has an accuracy of above 98% in detecting tumor areas.

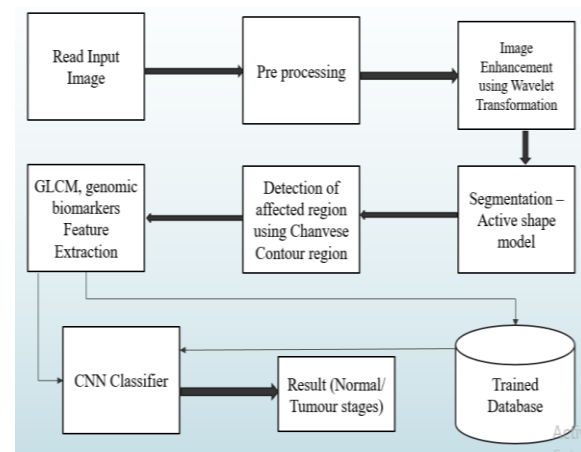


Fig 1 Block diagram of proposed system

Brain region extraction: In this study, we first apply a thresholding filter to the test image to remove any artefacts, such as bones and other body parts. The thresholding filter divides the test image into two parts based on a threshold that is manually chosen. The threshold is chosen via a trial-and-error analysis. The chosen threshold then performs well on all of the photos taken into account for the suggested investigation. Based on their pixels, the considered photos can be precisely separated. Additionally, we manually divided the portion of the photographs when the approach failed.

Modules Description: Training and testing are two of the elements in our proposed system. The system receives the cropped CT scan picture from the training module and performs pre-processing to improve the image. The features are retrieved and given to the SVM Classifier in the following phase. The CT image from the testing module is delivered to the pre-processing stage, and the next step is image segmentation to isolate the brain region and ROI. The third step is feature extraction and selection, which aims to identify the tumor's primary traits. The classifier, which determines whether cancer has been detected or not, is the final component.

A.PRE-PROCESSING:

Pre-processing includes following steps:

i. Input image:

The photos used as input in this case are tumor-filled JPEG images from a chest CT scan. The first image picked out of the file with the string filename. The user must choose the necessary brain CT scan image before proceeding with processing. Each image is then scaled down to 256*256.

ii. Median filtering:

RGB is the format of the input image. For further processing, it is initially transformed to a grayscale image. Then, a median filter with a mask size of 3*3 is used to remove noise from the CT images because it is one of the best ways to do so given that these pictures frequently have noise or artefacts from patient movements.

B.POST-PROCESSING:

Post-processing includes following steps:

i Brain Segmentation:

We separate the left and right brains from the CT image in this module. The CT image's seed point was first picked. We discovered the image's intensity value from that point. We contrast the intensity values of the current and adjacent pixels. Brains will be separated from the original image if the values of the neighboring pixels are similar to the seed value. From the CT picture, these similarity pixels will be separated. The last pixel is reached by continuing this technique. The segmentation of the Brains will come last. The chosen threshold value ranges from 0 to 180.

ii Lobe Segmentation:

Image segmentation often involves the use of watershed transformation. However, due to over segmentation and sensitivity to noise, its utility for automatic medical picture segmentation has been restricted. The segmentation algorithms for medical images have shown significant gains when prior shape knowledge is included. We suggest a unique technique that makes use of prior knowledge of shape and appearance to improve watershed segmentation. Internal markers are used in watershed to produce watershed lines along the gradient of the segmented image. Use the watershed

lines you obtained as outside markers. An individual internal marker and a portion of the background are present in each zone delineated by the external markers. Regions lacking markers are permitted to combine in watershed.

iii Feature Extraction:

In this procedure, the GLCM (Grey level co-occurrence matrix) is used to extract a total of 12 textural features from all of the database's photos. The categorization of tumors is then done using these features. The GLCM matrix only sums the instances in which a pixel in the input image with value *i* occurred in the given spatial relationship to a pixel with value *j*. Calculations of texture features employ the information in the GLCM to provide a measurement of the intensity variation at the target pixel.

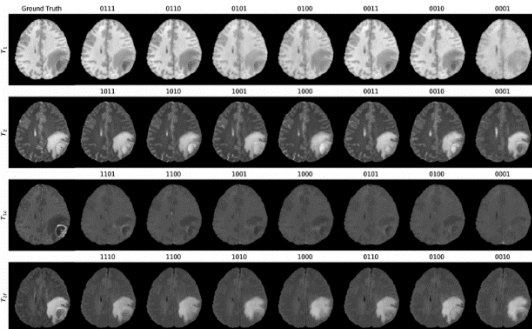


Fig 2 Input Image Selection

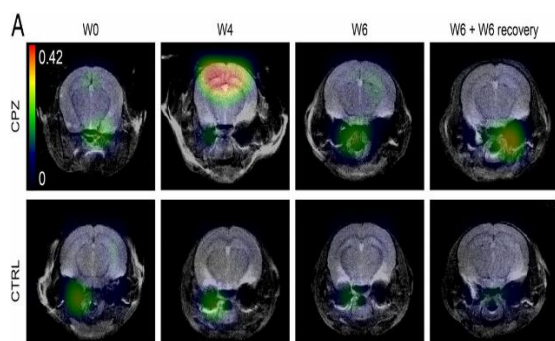


Fig 3 Pro-Processed Image

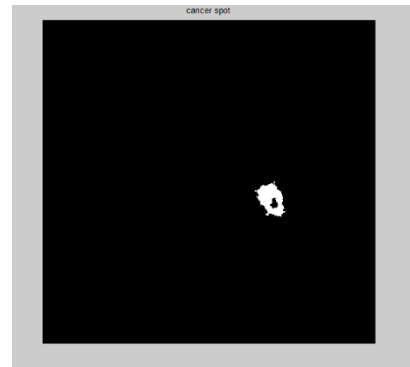


Fig 4 Tumor Spot Extracted

Average grey level, homogeneity, contrast, entropy, standard deviation, uniformity, smoothness, energy, and correlation. These attributes were taken from an image and include the following: Gray-Level Non Uniformity, Short Run Low Gray-Level Emphasis, and Long Run Low Gray-Level Emphasis.

IV. CONCLUSION

Recently, hyperpolarized [1-13C] brain tumors have been used in numerous mouse models of neurological disorders and neuro-inflammation, and it has been demonstrated that these models can yield useful information. Additionally, numerous hyperpolarized probes have been created and used in the healthy brain for the in vivo enzymatic assessment of a number of brain tumor pathways. The natural and practical next step for such probes is to turn to models of neurological illness. Clinical translation is already taking place in patients with TBI and healthy volunteers, and will likely follow in other patient groups in the next years, despite hurdles for hyperpolarized technology in the field of brain illnesses. Therefore, it would appear logical at this time to concentrate efforts on enhancing hardware, acquisition capability, processing pipelines, and hyperpolarized probes; these efforts should enable exploration of many Brain Tumor routes inside the human brain in both health and disease. A more effective methodology might enhance the long-term evaluation of therapeutic

response. The hyperpolarized ^{13}C technique presents an intriguing prospect to improve our comprehension of in vivo brain tumors and, in the future, to have an impact on clinical care in a variety of neurological illnesses when used in conjunction with other imaging modalities.

V. REFERENCES

- [1]Wu, Y.-H. *et al.* Jcs: An explainable Brain cancer diagnosis system by joint classification and segmentation. *arXiv preprint arXiv:2004.07054* (2020).
- [2]Ribbens, A., Hermans, J., Maes, F., Vandermeulen, D. & Suetens, P. Unsupervised segmentation, clustering, and groupwise registration of heterogeneous populations of brain MRI images. *IEEE transactions on medical imaging* 33, 201–224 (2013).
- [3]Gong, M., Liang, Y., Shi, J., Ma, W. & Ma, J. Fuzzy c-means clustering with local information and kernel metric for image segmentation. *IEEE transactions on image processing* 22, 573–584 (2012).
- [4]Kuo, J.-w. *et al.* Nested graph cut for automatic segmentation of high-frequency ultrasound images of the mouse embryo. *IEEE transactions on medical imaging* 35, 427–441 (2015).
- [5]Li, G. *et al.* Automatic liver segmentation based on shape constraints and deformable graph cut in ct images. *IEEE Transactions on Image Process.* 24, 5315–5329 (2015).
- [6]He, K., Gkioxari, G., Dollár, P. & Girshick, R. Mask r-cnn. In *Proceedings of the IEEE international conference on computer vision*, 2961–2969 (2017).
- [7]Ronneberger, O., Fischer, P. & Brox, T. U-net: Convolutional networks for biomedical image segmentation. In *International Conference on Medical image computing and computer-assisted intervention*, 234–241 (Springer, 2015).
- [8]Zhang, K., Zhang, L., Lam, K.-M. & Zhang, D. A level set approach to image segmentation with intensity inhomogeneity. *IEEE transactions on cybernetics* 46, 546–557 (2015).
- [9]Ding, K., Xiao, L. & Weng, G. Active contours driven by region-scalable fitting and optimized laplacian of gaussian energy for image segmentation. *Signal Process.* 134, 224–233 (2017).
- [10]Ding, K. & Xiao, L. A simple method to improve initialization robustness for active contours driven by local region fitting energy. *arXiv preprint arXiv:1802.10437* (2018).
- [11]Kim, W. & Kim, C. Active contours driven by the salient edge energy model. *IEEE Transactions on Image Process.* 22, 1667–1673 (2012).
- [12]Lecellier, F. *et al.* Region-based active contours with exponential family observations. *J. Math. Imaging Vis.* 36, 28 (2010).
- [13]Xu, T., Cheng, I. & Mandal, M. An improved fluid vector flow for cavity segmentation in chest radiographs. In *2010 20th International Conference on Pattern Recognition*, 3376–3379 (IEEE, 2010).
- [14]Ronfard, R. Region-based strategies for active contour models. *Int. journal computer vision* 13, 229–251 (1994).
- [15]Huang, R., Pavlovic, V. & Metaxas, D. N. A graphical model framework for coupling mrf and deformable models. In *Proceedings of the 2004 IEEE Computer Society Conference on Computer Vision and Pattern Recognition, 2004. CVPR 2004. vol. 2*, II–II (IEEE, 2004).